Accepted Manuscript

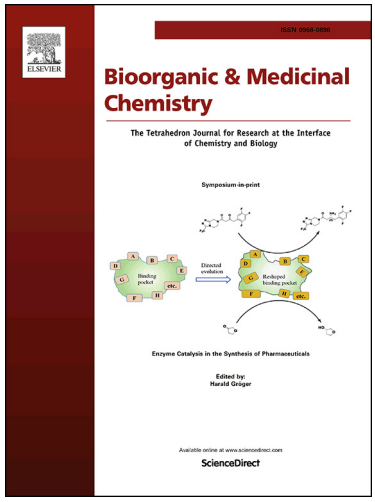

Discovery of 4,6-bis(benzyloxy)-3-phenylbenzofuran as a novel Pin1 inhibitor to suppress hepatocellular carcinoma via upregulating microRNA biogenesis

Xin Fan, Huaiyu He, Jiao Li, Guoyong Luo, Yuanyuan Zheng, Jian-Kang Zhou, Juan He, Wenchen Pu, Yun Zhao

PII: S0968-0896(19)30124-5
DOI: https://doi.org/10.1016/j.bmc.2019.04.028
Reference: BMC 14882

To appear in: *Bioorganic & Medicinal Chemistry*

Received Date: 22 January 2019
Revised Date: 9 April 2019
Accepted Date: 18 April 2019

Please cite this article as: Fan, X., He, H., Li, J., Luo, G., Zheng, Y., Zhou, J-K., He, J., Pu, W., Zhao, Y., Discovery of 4,6-bis(benzyloxy)-3-phenylbenzofuran as a novel Pin1 inhibitor to suppress hepatocellular carcinoma via upregulating microRNA biogenesis, *Bioorganic & Medicinal Chemistry* (2019), doi: https://doi.org/10.1016/j.bmc.2019.04.028

Graphical Abstract

To create your abstract, type over the instructions in the template box below.
Fonts or abstract dimensions should not be changed or altered.

Discovery of 4,6-bis(benzyloxy)-3-phenylbenzofuran as a novel Pin1 inhibitor to suppress hepatocellular carcinoma via upregulating microRNA biogenesis

Leave this area blank for abstract info.

Xin Fan, Huaiyu He, Jiao Li, Guoyong Luo, Yuanyuan Zheng, Jian-Kang Zhou, Juan He, Wenchen Pu and Yun Zhao

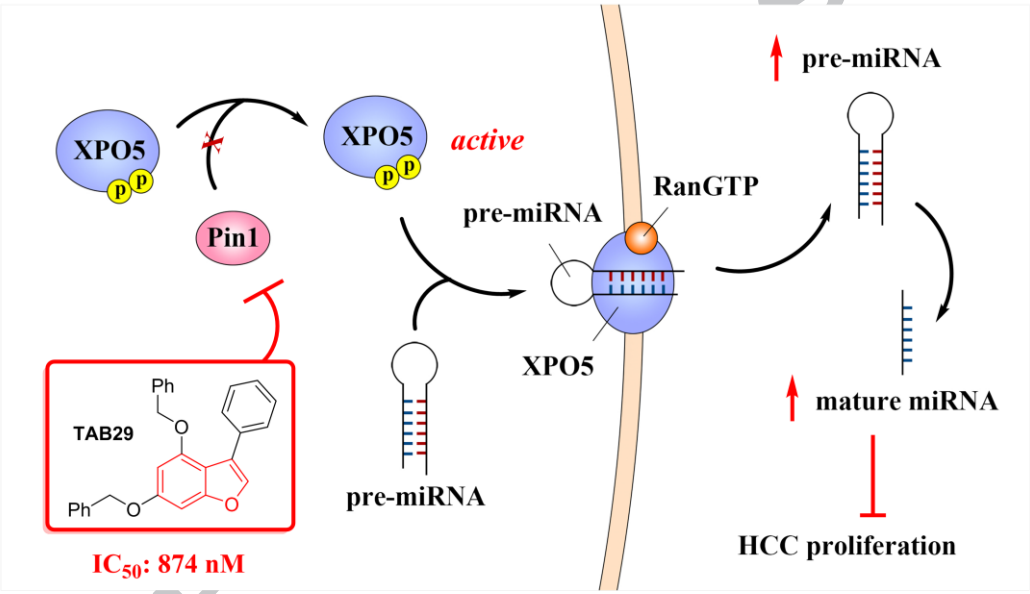

ELSEVIER

Bioorganic & Medicinal Chemistry
journal homepage: www.elsevier.com

Discovery of 4,6-bis(benzyloxy)-3-phenylbenzofuran as a novel Pin1 inhibitor to suppress hepatocellular carcinoma via upregulating microRNA biogenesis

Xin Fan[a,c], Huaiyu He[a,c], Jiao Li[a], Guoyong Luo[b], Yuanyuan Zheng[a], Jian-Kang Zhou[a], Juan He[a], Wenchen Pu[a,*] and Yun Zhao[a,*]

[a] *Key Laboratory of Bio-Resource and Eco-Environment of Ministry of Education, College of Life Sciences, Cancer Center, West China Hospital, Sichuan University, Chengdu 610041, China.*
[b] *Guiyang College of Traditional Chinese Medicine, Guiyang 550025, China.*

ARTICLE INFO

Article history:
Received
Revised
Accepted
Available online

Keywords:
Pin1
hepatocellular carcinoma
microRNA
benzofuran
XPO5

ABSTRACT

Peptidyl-prolyl *cis-trans* isomerase NIMA-interacting 1 (Pin1) participates in diverse cancer-associated signaling pathways, playing an oncogenic role in multiple human cancers, including hepatocellular carcinoma (HCC). Our recent works clarify that Pin1 modulates miRNAs biogenesis by interacting with ERK-phosphorylated exportin-5 (XPO5) and changing XPO5 conformation, giving a potential target for HCC treatment. Herein, we discover 4,6-bis(benzyloxy)-3-phenylbenzofuran (**TAB29**) as a novel Pin1 inhibitor that targets Pin1 PPIase domain. **TAB29** potently inhibits Pin1 activity with the IC_{50} value of 874 nM and displays an excellent selectivity toward Pin1 *in vitro*. Cell-based biological evaluation reveals that **TAB29** significantly suppresses cell proliferation of HCC cells through restoring the nucleus-to-cytoplasm export of XPO5 and upregulating mature miRNAs expression. Collectively, this work provides a promising small molecule lead compound for Pin1 inhibition, highlighting the therapeutic potential of miRNA-based treatment for human cancers.

1. Introduction

Peptidyl-prolyl *cis-trans* isomerase NIMA-interacting 1 (Pin1), belongs to the peptidyl-prolyl isomerase (PPIase) family, is the only known enzyme that catalyzes the *cis-trans* isomerization of phosphorylated Serine/Threonine-Proline (pS/T-P) motif of substrate.[1,2] Pin1 is widely overexpressed in human cancers and participates in diverse cancer-associated signaling pathways. For instance, Pin1 binds to CDK4-phosphoralated p53-R249S mutant and activates c-myc, facilitating the gain of function of mutant p53 in hepatocellular carcinoma (HCC).[3] Cullin3 (Cul3) substrate adaptor KLHL20 coordinates with the actions of CDK1/2 and Pin1 to mediate hypoxia-induced PML proteasomal degradation, potentiating prostate cancer progression.[4] Thus, Pin1 plays an oncogenic role in multiple human cancers.

Hepatocellular carcinoma (HCC) is the most critical type of primary liver cancer in adults, and is one of the leading causes of cancer death worldwide.[5] In HCC, microRNAs (miRNAs), a class of small noncoding RNAs that regulate gene expression by repressing protein translation or destabilizing target mRNAs,[6] are aberrantly downregulated.[7,8] Importantly, compromised miRNAs biogenesis is the reason for the downregulation of mature miRNAs.[9] During the process of miRNA biogenesis, exportin-5-mediated (XPO5-mediated) nucleus-to-cytoplasm export of precursor miRNA (pre-miRNA) is the rate-limiting step.[10-12] Recently, we have demonstrated that Pin1 changes the conformation of XPO5 phosphorylated by ERK at T345/S416/S497, prevents microRNAs biosynthesis, thereby contributing to HCC development.[13,14] Therefore, Pin1 is an attractive drug target for HCC treatment.

Increasing endeavor have been devoted to the investigation of Pin1 inhibition. Early stage small molecule Pin1 inhibitors, such as juglone, EGCG and PiB, have been discovered by low throughput screening and exhibited moderate Pin1-inhibitory activity.[15] The juglone analogue KPT-6566 covalently interacts with Pin1 and promotes its structural change and degradation, inhibiting cancer cell proliferation.[16] All-trans retinoic acid (ATRA) selectively inhibits and degrades active Pin1 in acute promyelocytic leukemia and breast cancer cells by directly binding to the Pin1 active site.[17] Recently, 6-*O*-benzylguanine derivative API-1 has been found to locate into Pin1 PPIase domain and

* Corresponding author. *E-mail addresses*: zhaoyun@scu.edu.cn (Y. Zhao), pu_vincent@scu.edu.cn (W. Pu)

[c] These authors contributed equally to this work.

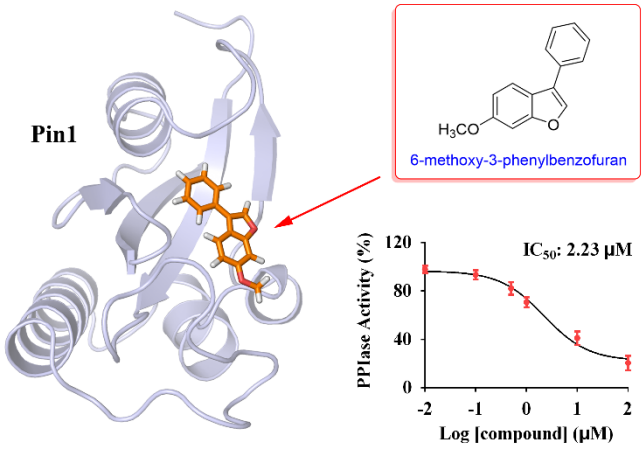

Fig. 1. 6-Methoxyl-3-phenylbenzofuran docked into PPIase domain of Pin1 and inhibited Pin1 activity with an IC_{50} value of 2.23 μM.

prevent its function both *in vitro* and *in vivo*.[18] However, to date, no Pin1 inhibitors have been applied to clinical treatment against solid tumor, including HCC, summoning an urgent need for novel Pin1 inhibitors.

Here, we identified 4,6-bis(benzyloxy)-3-phenylbenzofuran (**TAB29**) as a novel Pin1 inhibitor via computer-aided virtual screening and *in vitro* PPIase activity assay. **TAB29** was prepared with high yield via only two steps from commercially available materials. **TAB29** significantly suppressed HCC through restoring XPO5 function and upregulating miRNAs biogenesis, providing a valuable lead compound for Pin1 inhibition.

2. Results and Discussion

Based on the computer-aided virtual screening model established in our previous work,[18] we noticed that 6-methoxy-3-phenylbenzofuran was a lead structure targeting Pin1 PPIase domain (Fig. 1). Thus, we performed PPIase activity assay to characterize the Pin1 inhibitory function of 6-methoxy-3-phenylbenzofuran *in vitro*. In PPIase activity assay, a protease-coupled assay, the *p*-nitroaniline label added at the C terminus of peptide (Suc-AEPF-pNA) is subjected to cleavage by α-chymotrypsin after Pin1-induced *cis/trans* isomerization of Suc-AEPF-pNA, releasing free *p*-nitroaniline as a Pin1 activity reporter.[18] The data of *in vitro* PPIase activity assay demonstrated the Pin1 inhibitory activity of 6-methoxy-3-phenylbenzofuran with an IC_{50} value of 2.23 μM (Fig. 1). Thus, we planned to investigate the potential of 3-phenylbenzofuran derivatives as Pin1 inhibitors.

Firstly, a series of substituted 3-phenylbenzofurans, with diverse functional groups, were designed and submitted to chemical synthesis. Considering the commercial availability of starting materials and substrate scope of organic reactions, multiple synthetic strategies were utilized to prepare 3-phenylbenzofurans. Starting from benzophenones and dimethylacetamide, 3-phenylbenzofuran **TAB1-9** were afforded via copper-mediated cascade formation of furan O1-C2 and C2-C3 bonds (Scheme 1).[19] To prepare 5-methoxyl 3-phenylbenzofurans, 4-methoxyphenol and substituted 2-bromo-1-phenylethan-1-ones were used to conduct condensation and cyclization to obtain **TAB10-14** with 60-81% yields (Scheme 2). Furthermore, 5-hydroxyl 3-phenylbenzofuran **TAB15-19** were

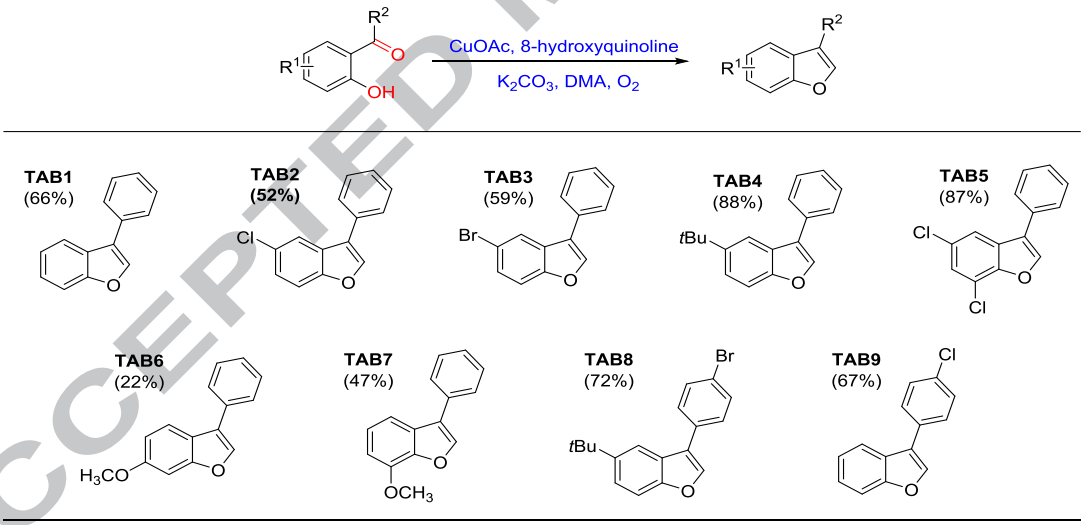

Scheme 1. Synthesis of **TAB1-9** from benzophenones and dimethylacetamide via copper-promoted cascade formation of furan O1-C2 and C2-C3 bonds.

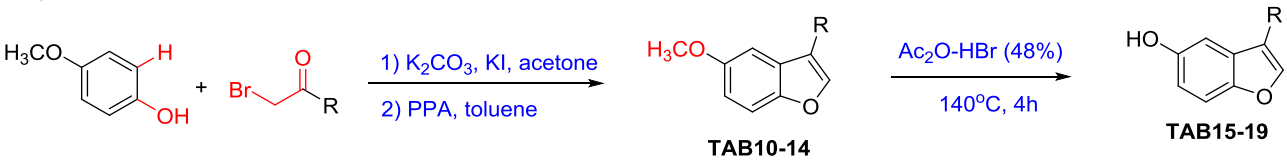

TAB10: R = phenyl (83%)
TAB11: R = 4-chlorophenyl (74%)
TAB12: R = 4-fluorophenyl (76%)
TAB13: R = 4-methylphenyl (60%)
TAB14: R = 3,4-dimethylphenyl (81%)

TAB15: R = phenyl (85%)
TAB16: R = 4-chlorophenyl (84%)
TAB17: R = 4-fluorophenyl (90%)
TAB18: R = 4-methylphenyl (80%)
TAB19: R = 3,4-dimethylphenyl (91%)

Scheme 2. Synthesis of 5-methoxyl or 5-hydroxyl 3-phenylbenzofurans (**TAB10-19**) from 4-methoxyphenol and substituted 2-bromo-1-phenylethan-1-ones.

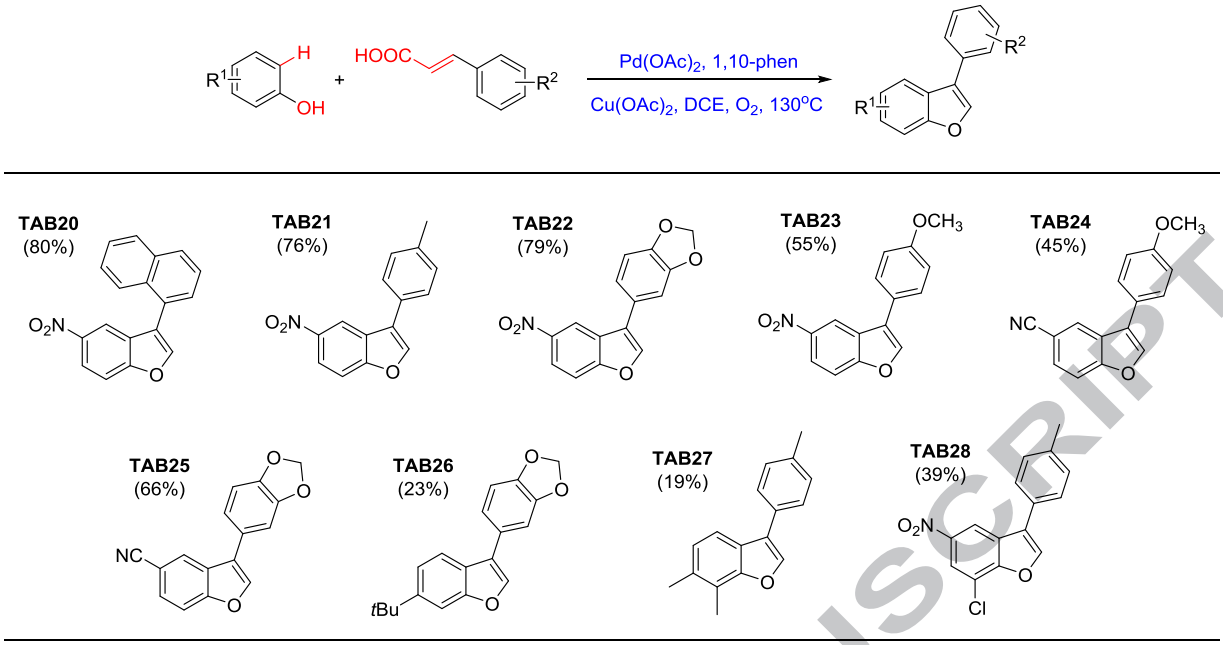

Scheme 3. Synthesis of **TAB20-28** from cinnamic acids through C-H olefination of phenols.

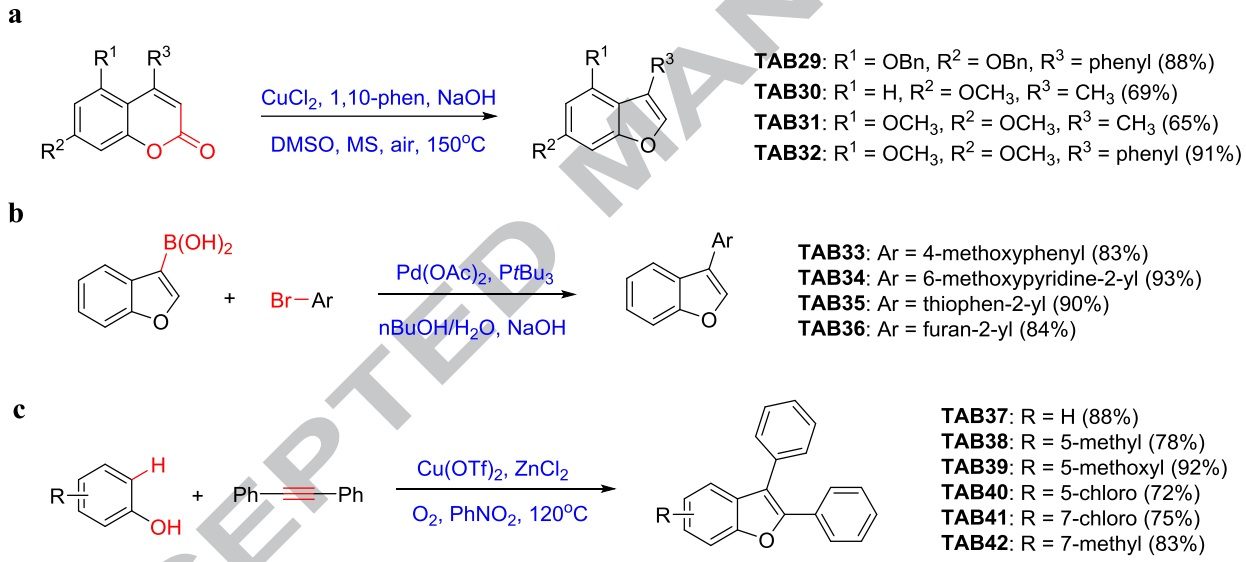

Scheme 4. Synthesis of **TAB29-42** from (a) 4-phenylcoumarins via copper-catalyzed decarboxylative intramolecular C-O coupling, (b) Suzuki coupling of heteroaryl bromides, (c) copper-catalyzed aerobic oxidative cyclization of phenols and alkynes.

synthesized by demethylation of corresponding 5-methoxyl 3-phenylbenzofurans with high yields (Scheme 2).[20] Selective palladium-catalyzed C-H olefination of phenol is favorable for the synthesis of 3-phenylbenzofurans with 5-nitro, 5-cyano or 6-alkyl groups.[21] Thus, **TAB20-28** were prepared under this protocol from cinnamic acids and phenols with acceptable yields (Scheme 3).

Our self-developed copper-catalyzed decarboxylative intramolecular C-O coupling is preferable for C-4- and/or C-6-substituted 3-phenlbenzofurans synthesis.[22] **TAB29-32** were smoothly afforded from corresponding 4-phenlycoumarins with 65-91% yields (Scheme 4a). To evaluate the influence of C-3 heteroaryl and C-2 phenyl substitutions of benzofurans, 3-heteroaryl benzofuran **TAB34-36** as well as **TAB33** were obtained via palladium-catalyzed Suzuki coupling of aryl bromides and benzofuran-3-ylboronic acid (Scheme 4b).[23] And then, to prepare 2,3-diphenylbenzofurans, phenols and alkynes were aerobic oxidative cyclized in the presence of copper species to afford **TAB37-42** (Scheme 4c).[24] Together, forty-two 3-arylbenzofuran compounds (**TAB1-42**) were successfully synthesized through a variety of synthetic methodologies.

With these compounds in hand, we further evaluated their potential binding affinity toward Pin1 PPIase domain via molecular docking and Pin1 inhibitory activity via *in vitro* PPIase activity assay. As in Table 1, **TAB29** exhibited the most potent Pin1 inhibitory function *in vitro* with 75.38% of Pin1 inhibition and the high predictive affinity toward PPIase domain with 57.02 GOLDScore.Fitness. **TAB29** exhibited stronger activity than juglone *in vitro* with the IC_{50} value of 0.874 μM (Fig. 2a). Furthermore, to identify the selectivity of **TAB29** against Pin1 protein, we conducted PPIase activity assay using other PPIases including Pin4, FKBP12 and cyclophilin A, which were expressed and purified from *E. coli.* system. The results indicated that **TAB29** was insensitive to Pin4, FKBP12 and cyclophilin A, showing excellent selectivity to Pin1 over other PPIases (Fig. 2b).

In order to give the binding mode of Pin1 and **TAB29**, we performed flexible docking based on the crystal structure of Pin1 (PDB ID: 3IKD). The result indicated that the oxygen of

Table 1. Pin1 inhibition of 3-arylbenzofurans at 10 μM in PPIase activity assay and their potential binding affinity toward PPIase domain in GOLD molecular docking.

Compound	Pin1 inhibition (%)	GOLD Score	Compound	Pin1 inhibition (%)	GOLDScore	Compound	Pin1 inhibition (%)	GOLDScore
Juglone	52.58	-						
TAB1	12.38	38.29	**TAB15**	28.02	55.86	**TAB29**	**75.38**	**57.02**
TAB2	19.16	40.21	**TAB16**	13.82	39.38	**TAB30**	65.08	52.83
TAB3	19.48	36.48	**TAB17**	23.76	52.94	**TAB31**	45.91	54.98
TAB4	10.97	22.67	**TAB18**	33.07	48.97	**TAB32**	69.58	59.17
TAB5	16.23	30.24	**TAB19**	27.82	34.32	**TAB33**	54.75	59.02
TAB6	59.53	56.84	**TAB20**	13.97	37.18	**TAB34**	34.83	55.82
TAB7	22.25	47.61	**TAB21**	32.62	39.27	**TAB35**	43.51	38.77
TAB8	28.87	54.83	**TAB22**	23.36	46.20	**TAB36**	22.18	50.32
TAB9	18.29	47.29	**TAB23**	43.73	62.01	**TAB37**	15.75	47.30
TAB10	26.98	40.88	**TAB24**	38.21	52.69	**TAB38**	13.86	35.33
TAB11	18.03	48.74	**TAB25**	46.87	54.71	**TAB39**	25.72	50.37
TAB12	30.74	39.58	**TAB26**	63.72	53.82	**TAB40**	22.91	43.45
TAB13	29.83	42.11	**TAB27**	64.64	43.58	**TAB41**	13.61	54.82
TAB14	23.67	52.84	**TAB28**	30.32	35.76	**TAB42**	19.63	45.90

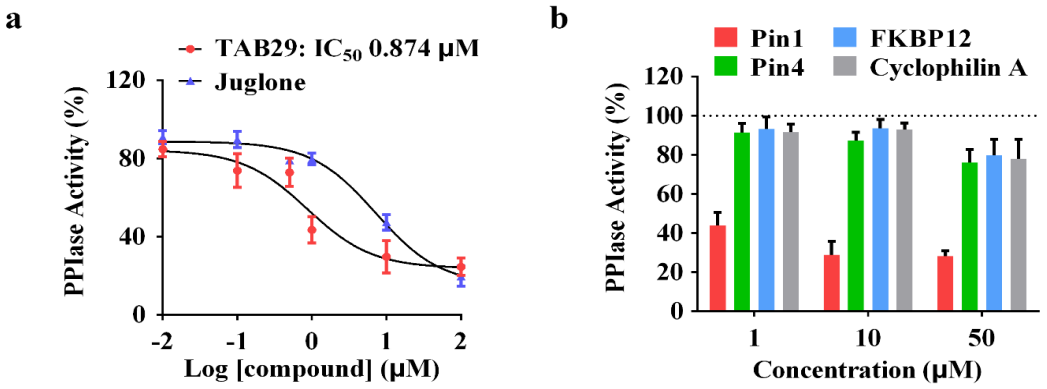

Fig. 2. TAB29 is a potent and selective Pin1 inhibitor. (a) PPIase activity assay of **TAB29** at varied concentrations using Pin1 as enzyme and juglone as positive control. Graphic data were run in duplicate and were shown as the means ± SD. (b) PPIase activity assay of **TAB29** at the concentration of 1, 10, 50 μM using Pin1, Pin4, Cyclophilin A or FKBP12 as enzyme. Graphic data were run in duplicate and were shown as the means ± SD.

benzyloxy group at C-6 position interacted with Ser114 amino acid residue through hydrogen bond (Fig. 3). Benzofuran motif associated with both Arg68 and Arg69 via cation-π interaction, while this interaction was also existed between the benzene ring of benzyloxy group at C-6 position and Arg69 residue (Fig. 3), giving potential structural basis for the interaction of Pin1 and **TAB29**.

To further evaluate the activity of the small molecular **TAB29** in HCC cells, the cell viability of HCC cells was detected by MTT assay. The results indicated **TAB29** inhibited cell proliferation of HCC cells with an IC_{50} value of 1.140 μM in SK-Hep-1 cells and 2.732 μM in SNU-423 cells (Fig. 4a and Table 2). Moreover, to check whether this anti-proliferative effect was under time- and dose- dependent manner, the cell viability of SK-Hep-1 cells was measured after 0, 24, 48, 72 and 96 hours of **TAB29** treatment at the concentrations of 5, 10 and 25 μM, respectively. The results showed the cell viability was decreased with the prolongation of inhibitor treatment time (Fig. 4b). The data of colony formation assay also confirmed the anti-proliferation activity of **TAB29** in HCC cells (Fig. 5). These data indicated the Pin1 inhibitor **TAB29** could effectively inhibit cell proliferation of HCC cells in a dose- and time-dependent manner.

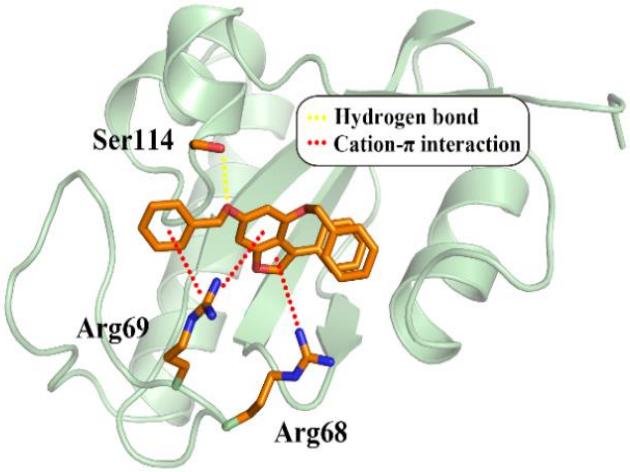

Fig. 3. Flexible docking of **TAB29** and Pin1 (PDB ID: 3IKD) in Discovery Studio software.

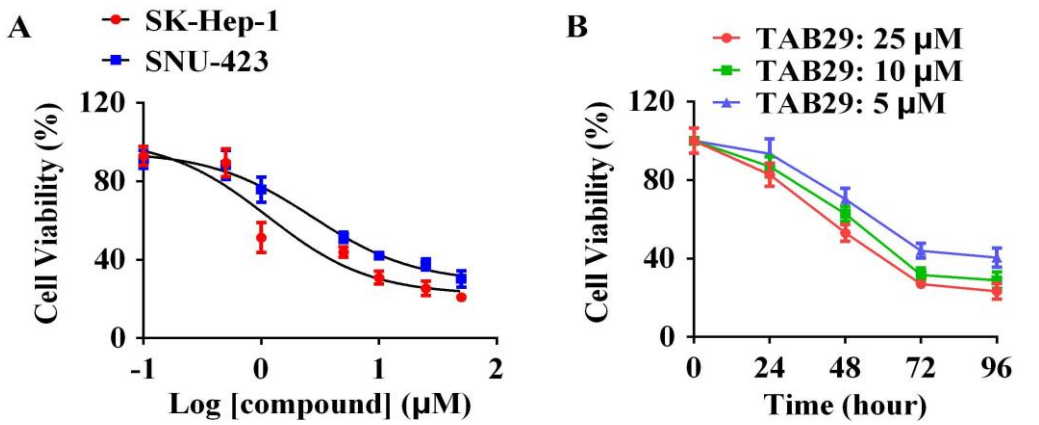

Fig. 4. TAB29 suppresses HCC cell proliferation. (a) MTT assay of **TAB29** at varied concentrations in SK-Hep-1 and SNU-423 cells. Graphic data were run in duplicate and were shown as the means ± SD. (b) MTT assay of **TAB29** in SK-Hep-1 at the concentrations of 5 (blue), 10 (green) and 25 μM (red) measured in the indicated times. Graphic data were run in duplicate and were shown as the means ± SD.

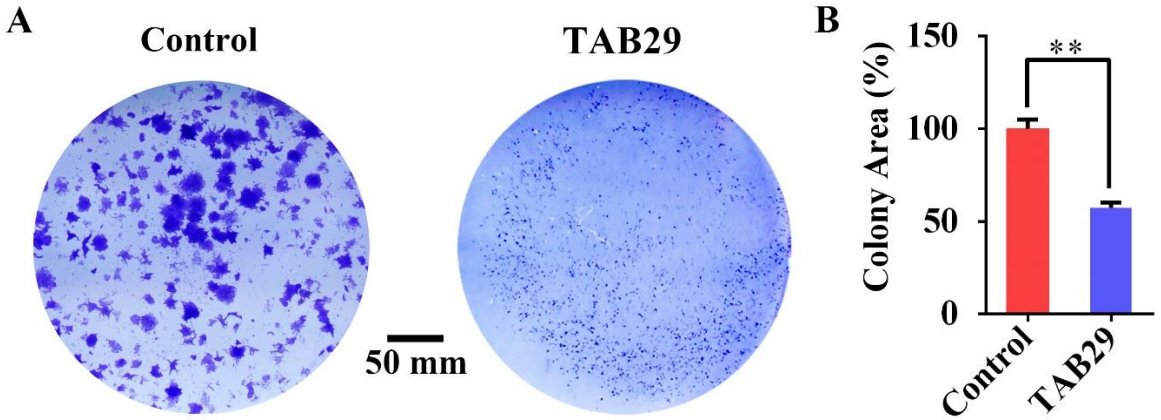

Fig. 5. TAB29 suppresses HCC colony formation. (A) The images of colony formation assay in SK-Hep-1 cells with or without **TAB29** (2.5 μM) treatment. (B) The quantification of colony formation assay in SK-Hep-1 cells with or without **TAB29** (2.5 μM) treatment. The data were normalized to the colony area of control. ** $P < 0.01$.

Table 2. The IC_{50} values of **TAB29** in MTT assay against SK-Hep-1 and SNU-423 cells.

Cell line	IC_{50} (μM)
SK-Hep-1	1.140
SNU-423	2.732

Our previous research suggested the nucleus-to-cytoplasm transport of XPO5 and pre-miRNAs was inhibited by Pin1-induced inactivation of XPO5: after ERK induced phosphorylation of XPO5, the conformation of phosphorylated XPO5 was changed by Pin1, leading to the reduction of miRNAs biogenesis;[13,14] Pin1 inhibition restored XPO5 exportation and upregulated miRNAs expression.[14,18] Thus, to evaluate the function of **TAB29** toward miRNAs biogenesis, confocal microscopy experiment and real-time quantitative PCR (qPCR) were performed in SK-Hep-1 cells. As in Fig. 6a, compared with DMSO-treated SK-Hep-1 cells, the cytoplasm distribution of XPO5 was significantly increased upon **TAB29** incubation, indicating **TAB29** could restore the nucleus-to-cytoplasm export of XPO5 in HCC cells. Furthermore, the results of qPCR showed **TAB29** could remarkably promote the biosynthesis of miRNAs (miR-122 and miR-29b) (Fig. 6b). It has been reported that delivery of miR-122, a liver-specific and dominant microRNA (about 70% of total miRNAs in normal liver cells), to a myc-driven mouse model of HCC strongly inhibits tumorigenesis.[25] Moreover, systemic administration of miR-29b significantly suppresses angiogenesis and tumorigenesis *in vivo*.[26] Owing to the tumor suppressive role of miR-122 and miR-29b, these results gave a potential mechanism for the anti-cancer activity of **TAB29**.

Broad pharmacological activity of benzofuran and widespread existence in nature have aroused people's attention. Studies have shown various biological activities of benzofuran, such as antitumor and antioxidant activities.[27,28] However, the mechanism of antitumor benzofurans remain obscure. In our study, we identified that 3-phenylbenzofuran **TAB29** suppressed HCC cell proliferation by targeting Pin1 isomerase (Fig. 2, 3, 4 and 5), which is significantly overexpressed in HCC and is the only enzyme catalyzing *cis-trans* isomerization of pS/T-P motif of substrate, suggesting a potential mechanism for the anticancer effect of benzofuran compounds.

We previously discovered a novel small-molecular Pin1 inhibitor API-1, exhibiting promising anti-HCC activity *in vitro* and *in vivo*.[18] However, unfavorable yield of API-1 (23% overall yield) via a four-steps method makes it difficult to conduct structural optimization and SAR study.[18] 3-Phenylbenzofuran-type Pin1 inhibitor **TAB29** has a concise chemical structure, which

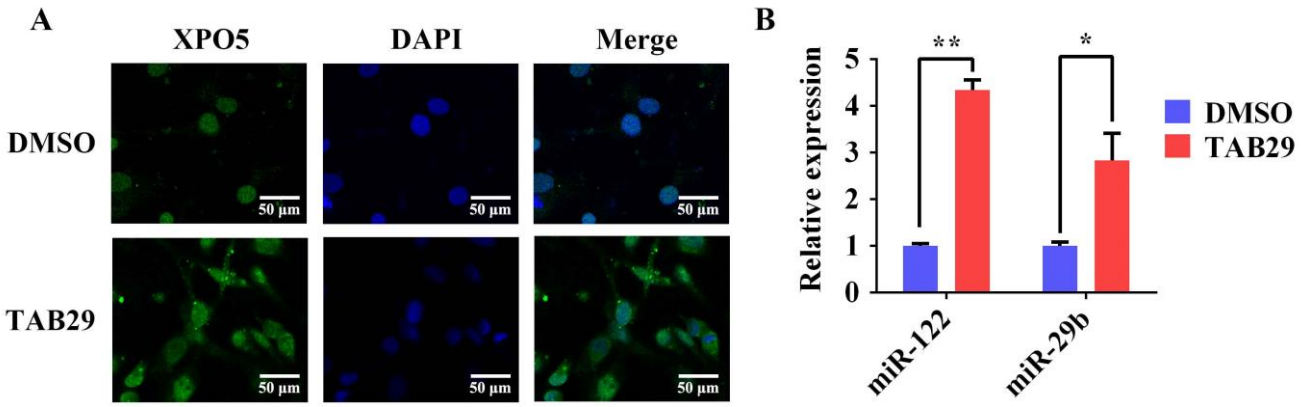

Fig. 6. TAB29 regulates miRNAs biogenesis via restoring XPO5 function. (a) Confocal microscopy of XPO5 nucleus/cytoplasm distribution in SK-Hep-1 cells with or without TAB29 (2.5 μM) treatment. (b) Mature miRNAs expression detected by quantitative PCR in SK-Hep-1 cells with or without TAB29 (2.5 μM) treatment. Graphic data were run in duplicate and were shown as the means ± SD. Statistical significance was determined by the Student t-test. * $P < 0.01$.

could be synthesized with 77% overall yield via a two-steps strategy including Pechmann reaction and subsequent decarboxylative intramolecular C-O coupling from commercial available materials (Scheme 4a), facilitating the SAR study and structural modification. Importantly, **TAB29**, with the IC_{50} value of 874 nM (Fig. 2a), performs a comparable Pin1 inhibitory function with other Pin1 inhibitors, providing a valuable lead structure for Pin1 inhibition.

HCC is one of the leading causes of cancer death worldwide. Although curative and pharmacological treatments have been developed in recent years, unfortunately, most individuals diagnosed with HCC are at advanced stage,[29] in which these treatments are less-effective,[30] miRNAs are globally downregulated in many tumors and tightly associated with tumor development, including HCC,[31,32] suggesting a potential miRNA-based therapy for HCC.[33,34] Our previous study showed that the conformation of phosphorylated XPO5 was changed by Pin1, resulting in the reduction of miRNA biogenesis and promoting HCC development.[13,14,18] In this study, we identified **TAB29** as a novel Pin1 inhibitor to enhance the biogenesis of tumor suppressor miRNAs (miR-122 and miR-29b) and suppresses HCC cell proliferation (Fig. 4, 5 and 6), providing experimental data to Pin1-targeted therapy for HCC and highlighting the therapeutic perspective of miRNA-based approach for human cancers.

3. Conclusion

This study screened out **TAB29** as a novel small-molecular Pin1 inhibitor with an IC_{50} value of 874 nM. **TAB29** had a potent and specific inhibitory activity toward Pin1 isomerase. MTT and colony formation assays confirmed that **TAB29** suppressed HCC cell proliferation in a dose- and time-dependent manner. Mechanistically, **TAB29** modulated the subcellular distribution of XPO5 and promoted mature miRNA biogenesis. Therefore, this work provided a promising lead compound for HCC treatment, highlighting the miRNA-targeted cancer therapy in human cancers.

4. Experimental

4.1. Chemistry

*4.1.1. Synthesis of **TAB1-9***

TAB1-9 were synthesized via the reported protocols.[19] In brief, a round-bottom flask was added 2-hydroxybenzophenones (0.252 mmol), copper acetate (0.123 mmol), 8-hydroxyquinoline (15 mg, 0.103 mmol), potassium carbonate (0.252 mmol) and anhydrous dimethylacetamide (2.5 mL). The mixture was stirred for 24 h at 140℃ under oxygen atmosphere. The mixture was cooled to room temperature and water (5.0 mL) was added. The resulting aqueous suspension was extracted with ethyl acetate (3 x 5 mL). The organic layer was then washed with water (15 mL) and brine (15 mL), dried over anhydrous sodium sulfate, and concentrated under reduced pressure. The crude product was purified by flash chromatography using ethyl acetate/hexane as eluent to give 3-phenylbenzofurans.

*3-Phenylbenzofuran (**TAB1**)*: yellow oil with 66% HPLC yields. ^{1}H NMR (400 MHz, $CDCl_3$) δ 7.87 (d, *J* = 7.7 Hz, 1H), 7.81 (s, 1H), 7.67 (d, *J* = 6.6 Hz, 2H), 7.54 (d, *J* = 7.1 Hz, 1H), 7.48 (t, *J* = 7.7 Hz, 2H), 7.38 (t, *J* = 6.9 Hz, 1H), 7.36-7.30 (m, 2H). ^{13}C NMR (100 MHz, $CDCl_3$) δ 155.9, 141.3, 132.0, 128.9, 127.5, 127.5, 124.5, 122.8, 122.3, 120.2, 111.7. HR-ESIMS: 217.0628 $[M+Na]^+$ (calc. for $C_{14}H_{10}NaO$, 217.0624).

*5-Chloro-3-phenylbenzofuran (**TAB2**)*: yellow oil with 52% HPLC yield. ^{1}H NMR (400 MHz, $CDCl_3$) δ 7.82 (s, 1H), 7.79 (s, 1H), 7.61 (d, *J* = 7.4 Hz, 2H), 7.51-7.45 (m, 3H), 7.38 (t, *J* = 7.4 Hz, 1H), 7.31 (dd, *J* = 8.7, 2.0 Hz, 1H). ^{13}C NMR (100 MHz, $CDCl_3$) δ 154.3, 142.5, 131.5, 129.1, 128.6, 127.9, 127.8, 127.4, 124.7, 122.2, 120.2, 112.7. HR-ESIMS: 251.0231 $[M+Na]^+$ (calc. for $C_{14}H_9{}^{35}ClNaO$, 251.0235).

*5-Bromo-3-phenylbenzofuran (**TAB3**)*: yellow oil with 59% HPLC yield. ^{1}H NMR (400 MHz, $CDCl_3$) δ 7.96 (s, 1H), 7.79 (s, 1H), 7.60 (d, *J* = 7.6 Hz, 2H), 7.49 (t, *J* = 7.6 Hz, 2H), 7.45-7.38 (m, 3H). ^{13}C NMR (100 MHz, $CDCl_3$) δ 154.7, 142.5, 131.3, 129.2, 128.7, 128.5, 127.7, 127.5, 123.2, 122.0, 116.2, 113.2. HR-ESIMS: 294.9727 $[M+Na]^+$ (calc. for $C_{14}H_9{}^{79}BrNaO$, 294.9729).

*5-tert-Butyl-3-phenylbenzofuran (**TAB4**)*: yellow oil with 88% HPLC yield. ^{1}H NMR (400 MHz, $CDCl_3$) δ 7.82 (s, 1H), 7.76 (s, 1H), 7.65 (d, *J* = 8.3 Hz, 2H), 7.54-7.37 (m, 5H), 1.42 (s, 9H), ^{13}C NMR (100 MHz, $CDCl_3$) δ 154.2, 146.2, 141.5, 132.3, 129.1, 127.6, 127.2, 126.0, 122.4, 116.3, 111.0, 34.8, 31.9. HR-ESIMS: 273.1254 $[M+Na]^+$ (calc. for $C_{18}H_{18}NaO$, 273.1250).

*5,7-Dichloro-3-phenylbenzofuran (**TAB5**)*: yellow oil with 87% HPLC. ^{1}H NMR (400 MHz, $CDCl_3$) δ 7.87 (s, 1H), 7.70 (d, *J* = 1.9 Hz, 2H), 7.62-7.52 (m, 2H), 7.51 (t, *J* = 7.6 Hz, 2H), 7.42 (d, *J* = 7.6 Hz, 1H), 7.38 (d, *J* = 1.9 Hz, 1H). ^{13}C NMR (100 MHz, $CDCl_3$) δ 151.5, 143.1, 132.9, 130.7, 129.1, 129.2, 128.6, 128.1, 127.6,

124.7, 119.6, 118.9. HR-ESIMS: 284.9842 [M+Na]$^+$ (calc. for $C_{14}H_8{}^{35}Cl_2NaO$, 284.9845).

*4-Methoxy-3-phenylbenzofuran (**TAB6**)*: yellow oil with 22% HPLC yield. ^{1}H NMR (400 MHz, $CDCl_3$) δ 7.72-7.63 (m, 4H), 7.51-7.35 (m, 3H), 7.07 (d, *J* = 2.3 Hz, 1H), 6.95 (dd, *J* = 8.7, 2.3 Hz, 1H), 3.86 (s, 3H). ^{13}C NMR (100 MHz, $CDCl_3$) δ 158.4, 156.7, 140.2, 132.2, 128.8, 127.4, 127.3, 122.1, 120.4, 112.1, 96.2, 55.7. HR-ESIMS: 247.0733 [M+Na]$^+$ (calc. for $C_{15}H_{12}NaO_2$, 247.0730).

*7-Methoxy-3-phenylbenzofuran (**TAB7**)*: yellow oil with 47% HPLC yield. ^{1}H NMR (400 MHz, $CDCl_3$) δ 7.82 (s, 1H), 7.66 (d, *J* = 8.1 Hz, 2H), 7.51-7.33 (m, 5H), 6.87 (d, *J* = 7.5 Hz, 1H), 4.04 (s, 3H). ^{13}C NMR (100 MHz, $CDCl_3$) δ 145.9, 145.3, 141.4, 132.0, 128.9, 128.1, 127.5, 127.5, 123.7, 122.6, 112.6, 106.6, 56.1. HR-ESIMS: 247.0731 [M+Na]$^+$ (calc. for $C_{15}H_{12}NaO_2$, 247.0730).

*3-(4-Bromophenyl)-5-tert-butylbenzofuran (**TAB8**)*: yellow oil with 72% HPLC yield. ^{1}H NMR (400 MHz, $CDCl_3$) δ 7.77 (s, 1H), 7.74 (d, *J* = 8.5 Hz, 1H), 7.64-7.58 (m, 2H), 7.51-7.40 (m, 4H), 1.39 (s, 9H). ^{13}C NMR (100 MHz, $CDCl_3$) δ 154.1, 146.4, 141.5, 132.1, 129.1, 124.3, 122.8, 121.5, 121.2, 121.1, 116.1, 111.2, 34.9, 31.9. HR-ESIMS: 351.0351 [M+Na]$^+$ (calc. for $C_{18}H_{17}{}^{79}BrNaO$, 351.0355).

*3-(4-Chlorophenyl)benzofuran (**TAB9**)*: yellow oil with 67% HPLC yield. ^{1}H NMR (400 MHz, $CDCl_3$) δ 7.82-7.77 (m, 2H), 7.60-7.54 (m, 3H), 7.46-7.43 (m, 2H), 7.41-7.32 (m, 2H), ^{13}C NMR (100 MHz, $CDCl_3$) δ 151.5, 143.0, 132.9, 130.4, 129.0, 128.7, 128.2, 127.6, 124.8, 119.3, 118.9. HR-ESIMS: 251.0231 [M+Na]$^+$ (calc. for $C_{14}H_9{}^{35}ClNaO$, 251.0235).

*4.1.2. Synthesis of **TAB10-19***

TAB10-19 were synthesized via the reported protocols.[20] In brief, potassium carbonate (5 mmol) and potassium iodide (5 mmol) were added to a mixture of 2-bromo-1-arylethanone (50 mmol), 4-methoxyphenol (5 mmol) and anhydrous acetone (60 mL). The mixture was stirred at room temperature in dark for 16 h under nitrogen atmosphere, and then was diluted with dichloromethane (120 mL). The solids were filtered off and the organic layer was washed with water, dried over anhydrous sodium sulfate and concentrated under reduced pressure. The crude products were directly used for the next reactions without further purification.

A mixture of 2-(4-methoxyphenoxy)-1-arylethanones (about 10 mmol), polyphosphoric acid (20 g), and toluene (60 mL) was refluxed for 6 h. The mixture was then cooled to room temperature, poured into water, and extracted with diethyl ether (3 x 50 mL). The organic extracts were dried over anhydrous sodium sulfate and evaporated under reduced pressure. The solid residue obtained was purified by silica gel column chromatography to give **TAB10-14**.

3-Aryl-5-methoxybenzofuran (2 mmol) was added to mixed solution (12 mL) of 48% hydrobromic acid and acetic anhydride (1:1, v/v). The mixture was refluxed at 140℃for 4 h and cooled to room temperature, neutralized with saturated sodium bicarbonate solution and extracted with diethyl ether (3 x 20 mL). The organic layer was washed with brine, dried over anhydrous sodium sulfate and evaporated under reduced pressure. The solid residue was purified by chromatography on silica gel column chromatography to give **TAB15-19**.

*5-Methoxy-3-phenylbenzofuran (**TAB10**)*: yellow oil with 83% HPLC yield. ^{1}H NMR (400 MHz, $CDCl_3$) δ 7.76 (s, 1H), 7.64-7.58 (m, 2H), 7.53-7.41 (m, 3H), 7.40-7.32 (m, 1H), 7.26 (d, *J* = 2.6 Hz, 1H), 6.96 (dd, *J* = 8.9, 2.6 Hz, 1H), 3.85 (s, 3H); ^{13}C NMR (100 MHz, $CDCl_3$) δ 156.4, 150.8, 142.2, 132.2, 129.1, 127.5, 127.3, 127.0, 122.4, 113.3, 112.2, 102.8, 56.0. HR-ESIMS: 247.0728 [M+Na]$^+$ (calc. for $C_{15}H_{12}NaO_2$, 247.0730).

*3-(4-Chlorophenyl)-5-methoxybenzofuran (**TAB11**)*: yellow oil with 74% HPLC yield. ^{1}H NMR (400 MHz, $CDCl_3$) δ 7.76 (s, 1H), 7.59-7.55 (m, 2H), 7.50-7.45 (m, 3H), 7.24 (d, *J* = 2.6 Hz, 1H), 7.01 (dd, *J* = 8.9, 2.6 Hz, 1H), 3.89 (s, 3H). ^{13}C NMR (100 MHz, $CDCl_3$): δ 156.4, 150.7, 142.3, 133.2, 130.6, 129.2, 128.6, 126.7, 121.4, 113.3, 112.3, 102.7, 56.0. HR-ESIMS: 281.0343 [M+Na]$^+$ (calc. for $C_{15}H_{11}{}^{35}ClNaO_2$, 281.0340).

*3-(4-Fluorophenyl)-5-methoxybenzofuran (**TAB12**)*: yellow oil with 76% HPLC yield. ^{1}H NMR (400 MHz, $CDCl_3$) δ 7.31 (s, 1H), 7.26-7.17 (m, 5H), 6.91 (t, *J* = 8.7 Hz, 2H), 6.85 (dd, *J* = 8.7, 2.6 Hz, 1H). HR-ESIMS: 265.0638 [M+Na]$^+$ (calc. for $C_{15}H_{11}FNaO_2$, 265.0636).

*5-Methoxy-3-(p-tolyl)benzofuran (**TAB13**)*: yellow oil with 60% HPLC yield. ^{1}H NMR (400 MHz, $CDCl_3$) δ 7.85 (s, 1H), 7.65 (d, *J* = 8.1 Hz, 2H), 7.56 (d, *J* = 8.9 Hz, 1H), 7.42-7.40 (m, 3H), 7.10 (dd, *J* = 8.9, 2.6 Hz, 1H), 3.97 (s, 3H), 2.54 (s, 3H). ^{13}C NMR (100 MHz, $CDCl_3$) δ 156.4, 150.9, 142.2, 137.3, 129.8, 129.3, 127.4, 127.3, 122.4, 113.2, 112.2, 103.1, 56.0, 21.3. HR-ESIMS: 261.0888 [M+Na]$^+$ (calc. for $C_{16}H_{14}NaO_2$, 261.0886).

*3-(3,4-Dimethylphenyl)-5-methoxybenzofuran (**TAB14**)*: yellow oil with 81% HPLC yield. ^{1}H NMR (400 MHz, $CDCl_3$) δ 7.45 (s, 1H), 7.16-7.02 (m, 5H), 6.76 (dd, *J* = 8.6, 2.4 Hz, 1H), 2.25 (s, 3H), 2.22 (s, 3H). HR-ESIMS: 275.1045 [M+Na]$^+$ (calc. for $C_{17}H_{16}NaO_2$, 275.1043).

*3-Phenylbenzofuran-5-ol (**TAB15**)*: yellow oil with 85% HPLC yield. ^{1}H NMR (400 MHz, $CDCl_3$) δ 7.76 (s, 1H), 7.61-7.58 (m, 2H), 7.47-7.43 (m, 2H), 7.39 (d, *J* = 9.0 Hz 1H), 7.37-7.34 (m, 1H), 7.24 (d, *J* = 2.4 Hz, 1H), 6.86 (dd, *J* = 9.0, 2.4 Hz, 1H), 4.88 (s, 1H). ^{13}C NMR (100 MHz, $CDCl_3$) δ 151.3, 150.6, 142.1, 131.7, 128.7, 127.1, 126.9, 121.9, 113.2, 112.0, 105.5. HR-ESIMS: 209.0594 [M-H]$^-$ (calc. for $C_{14}H_9O_2$, 209.0598).

*3-(4-Chlorophenyl)benzofuran-5-ol (**TAB16**)*: yellow oil with 84% HPLC yield. ^{1}H NMR (400 MHz, D_6-acetone) δ 8.05 (s, 1H), 7.69 (d, *J* = 8.4 Hz, 2H), 7.48 (d, *J* = 8.4 Hz, 2H), 7.40 (d, *J* = 9.0 Hz, 1H), 7.28 (d, *J* = 2.4 Hz, 1H), 6.93 (dd, *J* = 9.0, 2.4 Hz, 1H). ^{13}C NMR (100 MHz, D_6-acetone) δ 154.1, 150.3, 143.2, 132.6, 131.3, 129.2, 128.8, 126.8, 120.9, 113.8, 112.2, 104.9. HR-ESIMS: 243.0210 [M-H]$^-$ (calc. for $C_{14}H_8{}^{35}ClO_2$, 243.0208).

*3-(4-Fluorophenyl)benzofuran-5-ol (**TAB17**)*: yellow oil with 90% HPLC yield. ^{1}H NMR (400 MHz, $CDCl_3$) δ 7.59 (s, 1H), 7.28 (dd, *J* = 8.7, 5.5 Hz, 2H), 7.25 (d, *J* = 8.7 Hz, 1H), 7.11 (d, *J* = 2.7 Hz, 1H), 6.91 (t, *J* = 8.7 Hz, 2H), 6.84 (dd, *J* = 8.7, 2.7 Hz, 1H), 6.66 (s,1H). ^{13}C NMR (100 MHz, $CDCl_3$) δ 161.8 (d), 151.1, 150.5, 142.0, 128.4 (d), 127.5, 126.9, 121.0, 115.5 (d), 113.3, 112.1, 105.4. HR-ESIMS: 227.0501 [M-H]$^-$ (calc. for $C_{14}H_8FO_2$, 227.0503).

*3-p-Tolylphenylbenzofuran-5-ol (**TAB18**)*: yellow oil with 80% HPLC yield. ^{1}H NMR (400 MHz, D6-acetone) δ 7.96 (s, 1H), 7.55 (d, *J* = 7.8 Hz, 2H), 7.38 (d, *J* = 9.0 Hz, 1H), 7.31 (d, *J* = 2.4 Hz, 1H), 7.26 (d, *J* = 7.8 Hz, 2H), 6.94 (dd, *J* = 9.0, 2.4 Hz, 1H), 2.37

(s, 3H). ^{13}C NMR (100 MHz, D6-acetone) δ 153.9, 150.4, 142.4, 137.0, 129.8, 129.5, 127.3, 127.2, 122.0, 113.6, 112.0, 105.2, 20.8. HR-ESIMS: 223.0752 [M-H]$^-$ (calc. for $C_{15}H_{11}O_2$, 223.0754).

*3-(3,4-Dimethylphenyl)benzofuran-5-ol (**TAB19**)*: yellow oil with 91% HPLC yield. ^{1}H NMR (400 MHz, $CDCl_3$) δ 7.64 (s, 1H), 7.29-7.06 (m, 5H), 6.81 (dd, *J* = 8.7, 2.4 Hz, 1H), 2.23 (s, 3H), 2.20 (s, 3H). ^{13}C NMR (100 MHz, $CDCl_3$) δ 151.2, 150.6, 141.8, 136.9, 135.7, 129.9, 129.1, 128.3, 127.3, 124.5, 121.8, 113.0, 111.9, 105.6, 19.8, 19.5. HR-ESIMS: 237.0914 [M-H]$^-$ (calc. for $C_{16}H_{13}O_2$, 237.0911).

*4.1.3. Synthesis of **TAB20-28***

TAB20-28 were synthesized via the reported protocols.[21] In brief, to a screw cap reaction tube charged with a magnetic stir-bar, palladium (II) acetate (0.025 mmol), 1,10-phenonthroline (0.05 mmol), copper (II) acetate (0.25 mmol), phenols (0.75 mmol) and cinnamic acids (0.25 mmol) were added under air atmosphere. In the reaction tube, dichloroethane (4 mL) was added and oxygen was purged in the mixture for 15 min. Then the mixture was vigorously stirred in a preheated oil bath at 130℃ for 24h. After completion, the mixture was filtered through a celite with ethyl acetate as the washing solvent. The organic layer was washed with brine, dried over anhydrous sodium sulfate and evaporated under reduced pressure. The residue was purified by silica gel column chromatography to afford **TAB20-28**.

*3-(Naphthalen-1-yl)-5-nitrobenzofuran (**TAB20**)*: yellow solid with 80% HPLC yield. ^{1}H NMR (400 MHz, $CDCl_3$) δ 8.28-8.35 (m, 2H), 8.02-7.94 (m, 3H), 7.85 (m, 1H), 7.70 (d, *J* = 8.9 Hz, 1H), 7.64-7.54 (m, 3H), 7.48 (ddd, *J* = 8.3, 6.8, 1.4 Hz, 1H). ^{13}C NMR (100 MHz, $CDCl_3$) δ 158.2, 145.8, 144.6, 134.1, 132.1, 129.4, 129.1, 128.9, 128.2, 127.4, 126.9, 126.6, 125.7, 125.3, 122.0, 120.8, 117.80, 112.40. HR-ESIMS: 312.0635 [M+Na]$^+$ (calc. for $C_{18}H_{11}NNaO_3$, 312.0632).

*5-Nitro-3-(p-tolyl)benzofuran (**TAB21**)*: yellow solid with 76% HPLC yield. ^{1}H NMR (400 MHz, $CDCl_3$) δ 8.74 (d, *J* = 2.4 Hz, 1H), 8.28 (dd, *J* = 9.1, 2.4 Hz, 1H), 7.90 (s, 1H), 7.63 (d, *J* = 9.0 Hz, 1H), 7.54-7.50 (m, 2H), 7.35-7.32 (m, 2H), 2.44 (s, 3H). ^{13}C NMR (100 MHz, $CDCl_3$) δ 158.7, 144.6, 143.9, 138.5, 130.2, 127.6, 127.4, 125.4, 123.5, 120.6, 117.5, 112.3, 21.5. HR-ESIMS: 276.0635 [M+Na]$^+$ (calc. for $C_{15}H_{11}NNaO_3$, 276.0632).

*5-(5-Nitrobenzofuran-3-yl)benzo[d][1,3]dioxole (**TAB22**)*: yellow solid with 79% HPLC yield. ^{1}H NMR (400 MHz, $CDCl_3$) δ 8.71 (d, *J* = 2.4 Hz, 1H), 8.28 (dd, *J* = 9.0, 2.4 Hz, 1H), 7.85 (s, 1H), 7.61 (d, *J* = 9.0 Hz, 1H), 7.14-7.03 (m, 2H), 6.96 (d, *J* = 7.9 Hz, 1H), 6.05(s, 2H). ^{13}C NMR (100 MHz, $CDCl_3$) δ 158.6, 148.7, 148.0, 144.6, 143.7, 134.8, 127.4, 124.1, 121.4, 120.7, 117.3, 112.4, 109.3, 108.2, 101.6. HR-ESIMS: 306.0376 [M+Na]$^+$ (calc. for $C_{15}H_9NNaO_5$, 306.0373).

*3-(4-Methoxyphenyl)-5-nitrobenzofuran (**TAB23**)*: yellow solid with 55% HPLC yield. ^{1}H NMR (400 MHz, $CDCl_3$) δ 8.73 (d, *J* = 2.3 Hz, 1H), 8.28 (dd, *J* = 9.1, 2.3 Hz, 1H), 7.87 (s, 1H), 7.62 (d, *J* = 9.0 Hz, 1H), 7.59-7.53 (m, 2H), 7.08-7.04 (m, 2H), 3.89 (s, 3H). ^{13}C NMR (100 MHz, CDCl3) δ 159.9, 158.7, 144.6, 143.5, 129.0, 127.5, 123.2, 122.7, 120.6, 117.4, 115.0, 112.3, 55.6. HR-ESIMS: 292.0580 [M+Na]$^+$ (calc. for $C_{15}H_{11}NNaO_4$, 292.0581).

*3-(4-Methoxyphenyl)benzofuran-5-carbonitrile (**TAB24**)*: yellow solid with 45% HPLC yield. ^{1}H NMR (400 MHz, $CDCl_3$) δ 8.14 (t, *J* = 1.2 Hz, 1H), 7.83 (s, 1H), 7.62 (d, *J* = 1.2 Hz, 2H), 7.55-7.48 (m, 2H), 7.07-7.02 (m, 2H), 3.87 (s, 3H). ^{13}C NMR (100 MHz, $CDCl_3$) δ 159.8, 157.5, 142.7, 128.9, 128.3, 127.8, 125.9, 122.9, 122.2, 119.6, 114.9, 113.1, 107.1, 55.6. HR-ESIMS: 272.0685 [M+Na]$^+$ (calc. for $C_{16}H_{11}NNaO_2$, 272.0682).

*3-(Benzo[d][1,3]dioxol-5-yl)benzofuran-5-carbonitrile (**TAB25**)*: white solid with 66% HPLC yield. ^{1}H NMR (400 MHz, $CDCl_3$) δ 8.12 (t, *J* = 1.2 Hz, 1H), 7.82 (s, 1H), 7.65-7.60 (m, 2H), 7.09-7.02 (m, 2H), 6.95 (d, *J* = 7.9 Hz, 1H), 6.04 (s, 2H). ^{13}C NMR (100 MHz, $CDCl_3$) δ 157.5, 148.7, 147.9, 142.9, 128.4, 127.6, 125.8, 124.3, 121.4, 119.5, 113.2, 109.3, 108.12, 107.2, 101.8, 101.6. HR-ESIMS: 286.0477 [M+Na]$^+$ (calc. for $C_{16}H_9NNaO_3$, 286.0475).

*5-(6-tert-Butylbenzofuran-3-yl)benzo[d][1,3]dioxole (**TAB26**)*: white oil with 23% HPLC yield. ^{1}H NMR (400 MHz, $CDCl_3$) δ 7.73 (d, *J* = 8.3 Hz, 1H), 7.69 (s, 1H), 7.57 (d, *J* = 1.7 Hz, 1H), 7.38 (dd, *J* = 8.3, 1.7 Hz, 1H), 7.16-7.08 (m, 2H), 6.94-6.90 (m, 1H), 6.02 (s, 2H), 1.40 (s, 9H). ^{13}C NMR (100 MHz, $CDCl_3$) δ 156.3, 148.8, 148.3, 147.2, 140.8, 126.3, 124.1, 122.0, 121.0, 119.7, 109.0, 108.6, 108.1, 101.3, 35.1, 31.9. HR-ESIMS: 317.1146 [M+Na]$^+$ (calc. for $C_{19}H_{18}NaO_3$, 317.1149).

*6,7-Dimethyl-3-p-tolylbenzofuran (**TAB27**)*: white solid with 19% HPLC yield. ^{1}H NMR (400 MHz, $CDCl_3$) δ 7.77 (s, 1H), 7.59 (dd, *J* = 8.0, 4.1 Hz, 3H), 7.31 (d, *J* = 7.8 Hz, 2H), 7.16 (d, *J* = 8.0 Hz, 1H), 2.51 (s, 3H), 2.45 (s, 6H). ^{13}C NMR (100 MHz, $CDCl_3$) δ 155.5, 140.5, 137.2, 133.0, 129.7, 129.7, 127.4, 125.2, 124.1, 122.4, 120.4, 117.1, 21.4, 19.3, 11.8. HR-ESIMS: 259.1096 [M+Na]$^+$ (calc. for $C_{17}H_{16}NaO$, 259.1094).

*7-Chloro-5-nitro-3-p-tolylbenzofuran (**TAB28**)*: yellow solid with 39% HPLC yield. ^{1}H NMR (400 MHz, $CDCl_3$) δ 8.64 (d, *J* = 2.1 Hz, 1H), 8.32 (d, *J* = 2.1 Hz, 1H), 7.95 (s, 1H), 7.51-7.47 (m, 2H), 7.35-7.32 (m, 2H), 2.44 (s, 3H). ^{13}C NMR (100 MHz, $CDCl_3$) δ 154.6, 144.7, 144.4, 138.9, 130.3, 128.4, 127.7, 126.8, 124.4, 120.6, 118.3, 115.9, 21.5. HR-ESIMS: 310.0247 [M+Na]$^+$ (calc. for $C_{15}H_{10}{}^{35}ClNNaO_3$, 310.0242).

*4.1.4. Synthesis of **TAB29-32***

TAB29-32 were prepared via copper-catalyzed decarboxylative intramolecular C-O formation.[22] In brief, a 25 mL flask was charged with coumarins (1 mmol), cupric chloride (0.15 mmol), phenathroline (0.15 mmol), DMSO (10 mL) and 4 Å molecular sieve (300 mg). The reaction mixture was stirred and primarily heated to 110℃ for 1h. The temperature was then raised to 150℃ and maintained for 24 h. Keep the mixture exposing to air during all reaction time. After cooling to room temperature, hydrochloric acid (2 mol/L, 10 mL) and water (20 mL) were poured to terminate the reaction, which, simultaneously, brought about the generation of brown solid and bubble. The suspension was then extracted with chloroform (3 x 20 mL). The combined organic layer was washed in turn with water (20 mL) and brine (20 mL), dried over anhydrous magnesium sulfate, filtered and concentrated under reduced pressure. The solid residue obtained was purified by silica gel column chromatography.

*4,6-Bis(benzyloxy)-3-phenylbenzofuran (**TAB29**)*: white solid with 88% HPLC yield. ^{1}H NMR (400 MHz, $CDCl_3$) δ 7.57-7.62 (m, 2H), 7.51-7.45 (m, 3H), 7.41 (t, *J* = 7.4 Hz, 2H), 7.38-7.32 (m, 1H), 7.31-7.24 (m, 7H), 7.20-7.14 (m, 2H), 6.78 (d, *J* = 1.9 Hz, 1H), 6.54 (d, *J* = 1.9 Hz, 1H), 5.11 (s, 2H), 5.06 (s, 2H). ^{13}C NMR (100 MHz, $CDCl_3$) δ 158.1, 157.7, 153.7, 139.9, 136.7, 136.3, 132.1, 129.5, 128.6, 128.2, 128.1, 127.8, 127.6, 127.6, 127.1,

126.9, 122.8, 110.5, 96.4, 89.9, 70.6, 70.2. HR-ESIMS: 429.1461 $[M+Na]^+$ (calc. for $C_{28}H_{22}NaO_3$, 429.1462).

*6-Methoxy-3-methylbenzofuran (**TAB30**)*: white solid with 69% HPLC yield. ^{1}H NMR (400 MHz, $CDCl_3$) δ 7.37 (d, *J* = 8.5 Hz, 1H), 7.32 (d, *J* = 1.2 Hz, 1H), 6.99 (d, *J* = 2.2 Hz, 1H), 6.88 (dd, *J* = 8.5, 2.2 Hz, 1H), 3.85 (s, 3H), 2.21 (d, *J* = 1.3 Hz, 3H). HR-ESIMS: 185.0578 $[M+Na]^+$ (calc. for $C_{10}H_{10}NaO_2$, 185.0573).

*4,6-Dimethoxy-3-methylbenzofuran (**TAB31**)*: white solid with 65% HPLC yield. ^{1}H NMR (400 MHz, $CDCl_3$) δ 7.16 (d, *J* = 1.3 Hz, 1H), 6.57 (d, *J* = 1.9 Hz, 1H), 6.27 (d, *J* = 1.8 Hz, 1H), 3.86 (s, 3H), 3.83 (s, 3H), 2.30 (d, *J* = 1.2 Hz, 3H). HR-ESIMS: 215.0677 $[M+Na]^+$ (calc. for $C_{11}H_{12}NaO_3$, 215.0679).

*4,6-Dimethoxy-3-phenylbenzofuran (**TAB32**)*: white solid with 91% HPLC yield. ^{1}H NMR (400 MHz, $CDCl_3$) δ 7.65-7.60 (m, 2H), 7.49 (s, 1H), 7.43-7.37 (m, 2H), 7.36-7.31 (m, 1H), 6.69 (d, *J* = 2.0 Hz, 1H), 6.37 (d, *J* = 2.0 Hz, 1H), 3.87 (s, 3H), 3.81 (s, 3H). ^{13}C NMR (100 MHz, $CDCl_3$) δ 159.1, 157.8, 154.6, 139.8, 132.3, 129.2, 127.9, 127.0, 122.7, 109.7, 94.5, 88.2, 55.7, 55.3. HR-ESIMS: 277.0837 $[M+Na]^+$ (calc. for $C_{16}H_{13}NaO_3$, 277.0836).

*4.1.5. Synthesis of **TAB33-36***

TAB33-36 were synthesized via the reported protocols.[23] In brief, in an argon-filled glove box, to a 25 mL Schlenk tube was charged with palladium (II) acetate (0.010 mmol), tributylphosphonium tetrafluoroborate (0.012 mmol), heteroaryl bromide (0.50 mmol), organoboronic acid (0.60 mmol), n-dodecane (40 μL) and n-butanol (2.80 mL). The mixture was prestirred at room temperature for 15 min, and then a solution of sodium hydroxide (0.85 mmol) in 0.68 mL of degassed water was added to initiate the Suzuki reaction. The Schlenk tube was capped tightly and the reaction mixture was stirred vigorously at room temperature until the heteroaryl bromide was fully consumed. At the end of the reaction, the organic phase was separated and the aqueous phase was further extracted with ether (3 x 3 mL). The combined organic extracts were concentrated under reduced pressure. The resulting residue was purified by silica gel column chromatography to obtain **TAB33-36**.

*3-(4-Methoxyphenyl)benzofuran (**TAB33**)*: yellow oil with 83% HPLC yield. ^{1}H NMR (400 MHz, $CDCl_3$) δ 7.84-7.80 (m, 1H), 7.75 (s, 1H), 7.59-7.54 (m, 3H), 7.36-7.30 (m, 2H), 7.04-7.01 (m, 2H), 3.87 (s, 3H). ^{13}C NMR (100 MHz, $CDCl_3$) δ 160.6, 156.5, 142.4, 129.7, 126.3, 124.6, 123.5, 122.3, 121.3, 114.7, 111.5, 55.8. HR-ESIMS: 247.0732 $[M+Na]^+$ (calc. for $C_{15}H_{12}NaO_2$, 247.0730).

*2-(Benzofuran-3-yl)-6-methoxypyridine (**TAB34**)*: yellow oil with 93% HPLC yield. ^{1}H NMR (400 MHz, $CDCl_3$) δ 8.34-8.31 (m, 1H), 8.10 (s, 1H), 7.63 (dd, *J* = 8.3, 7.3 Hz, 1H), 7.56-7.54 (m, 1H), 7.37-7.34 (m, 2H), 7.29 (dd, *J* = 7.3, 0.7 Hz, 1H), 6.69 (d, *J* = 8.3 Hz, 1H), 4.09 (s, 3H). ^{13}C NMR (100 MHz, $CDCl_3$) δ 164.0, 156.2, 149.8, 144.1, 139.9, 125.8, 124.7, 123.3, 122.3, 121.9, 113.4, 111.7, 109.0, 53.6. HR-ESIMS: 248.0685 $[M+Na]^+$ (calc. for $C_{14}H_{11}NNaO_2$, 248.0682).

*3-(Thiophen-3-yl)benzofuran (**TAB35**)*: colorless oil with 90% HPLC yield. ^{1}H NMR (400 MHz, $CDCl_3$) δ 7.93-7.90 (m, 1H), 7.86 (s, 1H), 7.57-7.54 (m, 1H), 7.40-7.33 (m, 4H), 7.18-7.15 (m, 1H). ^{13}C NMR (100 MHz, $CDCl_3$) δ 155.7, 141.2, 133.5, 127.8, 126.1, 125.0, 124.4, 124.5, 123.3, 120.6, 116.4, 111.8. HR-ESIMS: 223.0185 $[M+Na]^+$ (calc. for $C_{12}H_8NaOS$, 223.0189).

*3-Furan-2-yl-benzofuran (**TAB36**)*: colorless oil with 84% HPLC yield. ^{1}H NMR (400 MHz, $CDCl_3$) δ 7.98 (s, 1H), 7.93-7.89 (m, 1H), 7.56-7.50 (m, 2H), 7.41-7.32 (m, 2H), 6.68-6.67 (m, 1H), 6.55-6.53 (m, 1H). ^{13}C NMR (100 MHz, CDCl3) δ 155.5, 147.1, 141.4, 140.9, 124.7, 124.6, 123.1, 120.7, 113.5, 111.7, 111.2, 106.0. HR-ESIMS: 207.0419 $[M+Na]^+$ (calc. for $C_{12}H_8NaO_2$, 207.0417).

*4.1.6. Synthesis of **TAB37-42***

TAB37-42 were synthesized via the reported protocols.[24] In brief, in a 20 mL Schlenk tube was charged with phenol (1.5 mmol), 1,2-diphenylethyne (1.0 mmol), zinc chloride (1.5 mmol), copper (II) triflate (0.1 mmol) and nitrobenzene (2 mL) under oxygen atmosphere. The mixture was heated at 120℃, and the reaction was allowed to stir for 24 h. After reaction completion, the mixture was washed with brine and extracted with ethyl acetate. The organic layer was dried with anhydrous magnesium sulfate, concentrated under reduced pressure and purified by silica gel column chromatography to give **TAB37-42**.

*2,3-Diphenylbenzofuran (**TAB37**)*: yellow oil with 88% HPLC yield. ^{1}H NMR (400 MHz, $CDCl_3$) δ 7.65-7.67 (m, 2H), 7.55 (d, *J* = 8.0Hz, 1H), 7.44-7.51 (m, 5H), 7.38-7.41 (m, 1H), 7.28-7.34 (m, 4H), 7.23 (t, *J* = 8.0 Hz, 1H). ^{13}C NMR (100 MHz, $CDCl_3$) δ 154.0, 150.6, 132.9, 130.7, 130.3, 129.8, 129.0, 128.4, 128.4, 127.7, 127.1, 124.7, 122.9, 120.1, 117.5, 111.1. HR-ESIMS: 293.0939 $[M+Na]^+$ (calc. for $C_{20}H_{14}NaO$, 293.0937).

*5-Methyl-2,3-diphenylbenzofuran (**TAB38**)*: yellow oil with 78% HPLC yield. ^{1}H NMR (400 MHz, $CDCl_3$) δ 7.64-7.64 (m, 2H), 7.36-7.47 (m, 6H), 7.25-7.26 (m, 4H), 7.09-7.11 (m, 1H), 2.38 (s, 3H). ^{13}C NMR (100 MHz, CDCl3) δ 152.6, 150.8, 133.2, 132.5, 130.9, 130.5, 129.9, 129.2, 128.5, 128.3, 127.7, 127.2, 126.1, 119.9, 117.6, 110.7, 21.5. HR-ESIMS: 307.1092 $[M+Na]^+$ (calc. for $C_{21}H_{16}NaO$, 307.1094).

*5-Methoxy-2,3-diphenylbenzofuran (**TAB39**)*: yellow solid with 92% HPLC yield. ^{1}H NMR (400 MHz, $CDCl_3$) δ 7.62 (d, *J* = 8.0Hz, 2H), 7.39-7.49 (m, 6H), 7.27-7.29 (m, 3H), 6.91-6.93 (m, 2H), 3.78 (s, 3H). ^{13}C NMR (100 MHz, $CDCl_3$) δ 156.3, 151.4, 149.1, 133.0, 130.8, 130.7, 129.8, 129.1, 128.4, 128.3, 127.6, 127.0, 117.8, 113.6, 111.7, 102.3, 56.0. HR-ESIMS: 323.1046 $[M+Na]^+$ (calc. for $C_{21}H_{16}NaO_2$, 323.1043).

*5-Chloro-2,3-diphenylbenzofuran (**TAB40**)*: orange solid with 72% HPLC yield. ^{1}H NMR (400 MHz, $CDCl_3$) δ 7.64-7.61 (m, 2H), 7.46-7.40 (m, 7H), 7.29-7.24 (m, 4H). ^{13}C NMR (100 MHz, $CDCl_3$) δ 152.4, 152.0, 132.2, 131.7, 130.2, 129.7, 129.1, 128.5, 128.0, 127.1, 124.9, 119.6, 117.2, 112.1. HR-ESIMS: 327.0542 $[M+Na]^+$ (calc. for $C_{20}H_{13}{}^{35}ClNaO$, 327.0548).

*7-Chloro-2,3-diphenylbenzofuran (**TAB41**)*: orange solid with 75% HPLC yield. ^{1}H NMR (400 MHz, $CDCl_3$) δ 7.76-7.72 (m, 2H), 7.54-7.48 (m, 5H), 7.43-7.41 (m, 1H), 7.38-7.36 (m, 4H), 7.21 (t, *J* = 8.0 Hz, 1H). ^{13}C NMR (100 MHz, $CDCl_3$) δ 151.5, 149.8, 132.4, 131.9, 130.1, 129.7, 129.1, 128.8, 128.5, 127.9, 127.2, 124.8, 123.8, 118.5, 118.0, 116.6. HR-ESIMS: 327.0549 $[M+Na]^+$ (calc. for $C_{20}H_{13}{}^{35}ClNaO$, 327.0548).

*7-Methyl-2,3-diphenylbenzofuran (**TAB42**)*: yellow solid with 83% HPLC yield. ^{1}H NMR (400 MHz, $CDCl_3$) δ 7.68-7.66 (m, 2H), 7.50-7.48 (m, 2H), 7.43 (t, *J* = 8.0 Hz, 2H), 7.38-7.37 (m, 1H), 7.32-7.25 (m, 4H), 7.13-7.11 (m, 2H), 2.61 (s, 3H). ^{13}C NMR (100 MHz, $CDCl_3$) δ 153.2, 150.3, 133.2, 131.0, 129.9, 129.8,

129.0, 128.5, 128.2, 127.6, 127.1, 125.7, 123.1, 121.4, 117.8, 117.6, 15.1. HR-ESIMS: 307.1097 $[M+Na]^+$ (calc. for $C_{21}H_{16}NaO$, 307.1094).

4.2. Computer-aided virtual screening and flexible docking

The computer-aided virtual screening and flexible docking calculation were performed by using the crystal structures of Pin1 (PDB ID: 3IKD) via GOLD docking and flexible docking protocols in Discovery Studio v3.1 software by using default parameters. The images of molecular docking were processed by PyMOL v1.8 software.

4.3. Preparation of recombinant proteins

Full-length Pin1 sequences with N-terminal 6 His tag followed by a thrombin cleavage site were subcloned into pET28 vector. In *E. coli* cells, protein expressions were induced by IPTG overnight at 16℃. The cells were then pelleted by centrifugation at 4000 rpm for 15 minutes and resuspended in 20 mL buffer (20 mM Tris-HCl, 150 mM NaCl, 25 mM imidazole pH 8.0). His-tag proteins were purified by nickel-affinity chromatography followed by thrombin cleavage. The proteins were further purified by size-exclusion chromatography using a Superdex 75 column (GE Healthcare).

4.4. PPIase activity assay

The typical PPIase activity assay was established by Jiang et. al.[35] and described in our previous work.[18] In brief, a typical PPIase activity assay (total volume of 150 μL) involves PPIases (80 nmol/L), *a*-chymotrypsin (6 mg/mL, Sigma), Suc-AEPF-pNA (50 μmol/L, Abcam), and test samples for reaction. Sample and PPIase protein were preincubated for 10 minutes, and the mixture was added to the reaction buffer containing *a*-chymotrypsin. The reaction was initiated by the addition of the Suc-AEPF-pNA, and the reaction progress was monitored at 390 nm on Thermo Scientific Varioskan Flash Multimode Reader at 4℃ for 180 seconds. The results of the Pin1 inhibition (%) in Table 1 were calculated by the following formula based on the OD values of tests at the time of 180s:

$$\text{Pin1 inhibition (\%)} = (OD_{Pin1}-OD_{inhibitor})/(OD_{Pin1}-OD_{abs})*100$$

OD_{Pin1} is the value of assay with Pin1 pretreated with vehicle. $OD_{inhibitor}$ is the value of assay with Pin1 pretreated with inhibitor. OD_{abs} is the value of assay in the absence of Pin1, inhibitor and vehicle.

4.5. Cell culture

SK-Hep-1 cells were cultured in DMEM medium supplemented with 10% fetal bovine serum (FBS). SNU-423 cells were cultured in RPMI 1640 medium with 10% FBS at 37℃ in a 5% CO_2 incubator.

4.6. Cell viability assay

HCC cells were seeded in a 96-well culture plate and allowed to grow for 24 hours in DMEM or RPMI 1640 medium supplemented with 10% fetal bovine serum and 1% penicillin/streptomycin sulfate. The cells were then treated with samples or vehicle and incubated in a 5% CO_2 incubator for indicated time. At the end of incubation, 10 μL of MTT stock solution (5 mg/mL) was added into each well. The plate was continued to be incubated at 37℃ for 4 hours before the medium was removed. Then, DMSO (100 μL) was added into each well, followed by thorough shaking. The absorbance of the formazan product was measured at 570 nm on Thermo Scientific Varioskan Flash Multimode Reader. The IC_{50} value was obtained by fitting dose-response data to a three parametric nonlinear regression model using GraphPad Prism 6.0 software.

4.7. Colony formation assay

SK-Hep-1 cells were seeded in a 6-well culture plate and allowed to grow for 24 hours in DMEM medium supplemented with 10% FBS and 1% penicillin/streptomycin sulfate. The cells were then treated with **TAB29** (2.5 μM) or vehicle and incubated in a 5% CO_2 incubator. After 7 days, the cells were dyed with crystal violet solution (0.5%) for 20 minutes. After removing crystal violet solution, the cells were washed by water and colony formation was recorded by high-resolution scanner.

4.8. Confocal microscopy

SK-Hep-1 cells were plated in a 6-well plate and treated with **TAB29** (2.5 μM) or vehicle control at 37℃ for 36 hours. For confocal microscopy, cells after treatments were fixed in 4% paraformaldehyde, permeabilized with 0.5% Triton X-100, blocked with 5% bovine serum albumin, and then incubated with anti-XPO5 at 4℃ overnight, followed by incubation with the appropriate secondary antibody. Nuclei were stained with DAPI before mounting. Confocal fluorescence images were captured using Leica TCS SP5 II confocal spectral.

4.9. Real-time quantitative PCR

The primers for miR-122 (catalog number: MQPS0000467-1-100) were ordered from RiboBio (Guangzhou, China). The sequences of primers for miR-29b were showed as Table S1 in Supplementary Information. SK-Hep-1 cells were plated in a 6-well plate and treated with **TAB29** (2.5 μM) or vehicle control at 37℃ for 36 hours. Total RNA was isolated by TRIzol Reagent (Thermo fisher) according to manufacturer's instruction. The concentrations of total RNAs were determined by Thermo NanoDrop 2000 UV-Vis spectrophotometer. cDNAs were generated from total RNAs by cDNA Reverse Transcription kit (Thermo fisher), and the microRNA (miRNA) level was determined by Applied Biosystems StepOne Plus Real-Time PCR Systems with SYBR Green reagent (Thermo fisher). Small endogenous nucleolar RNU6 was used as control for miRNA normalization.

Acknowledgments

This work was supported by National Natural Science Foundation of China (No.81702980 to W.P.), China Postdoctoral Science Foundation (No.2018M640925 to W.P.) and Post-Doctor Research Project, West China Hospital, Sichuan University (No.2018HXBH014 to W.P.).

Appendix A. Supplementary data

Supplementary data to this article can be found online at

References

1. Yeh ES, Means AR. PIN1, the cell cycle and cancer. *Nat Rev Cancer*. 2007;7:381-388.
2. Lu KP, Hanes SD, Hunter TA. A human peptidyl-prolyl isomerase essential for regulation of mitosis. *Nature*. 1996;380:544-547.

3. Liao P, Zeng SX, Zhou X, et al. Mutant p53 gains its function via c-myc activation upon CDK4 phosphorylation at serine 249 and consequent PIN1 binding. *Mol Cell.* 2017;68:1134-1146.
4. Yuan WC, Lee YR, Huang SF, et al. A Cullin3-KLHL20 ubiquitin ligase-dependent pathway targets PML to potentiate HIF-1 signaling and prostate cancer progression. *Cancer Cell.* 2011;20:214-228.
5. Bray F, Ferlay J, Soerjomataram I, Siegel RL, Torre LA, Jemal A. Global cancer statistics 2018: GLOBOCAN estimates of incidence and mortality worldwide for 36 cancers in 185 countries. *CA Cancer J Clin.* 2018;68:394-424.
6. Hata A, Lieberman J. Dysregulation of microRNA biogenesis and gene silencing in cancer. *Sci Signal.* 2015;8:re3
7. Calin GA, Croce CM. MicroRNA signatures in human cancers. *Nat Rev Cancer*. 2006;6:857-866.
8. Wong CM, Wong CC, Lee JM, Fan DN, Au SL, Ng IO. Sequential alterations of microRNA expression in hepatocellular carcinoma development and venous metastasis. *Hepatology*. 2012;55:1453-1461.
9. Lee EJ, Baek M, Gusev Y, Brackett DJ, Nuovo GJ, Schmittgen TD. Systematic evaluation of microRNA processing patterns in tissues, cell lines, and tumors. *RNA.* 2008;14:35-42.
10. Lin S, Gregory RI. MicroRNA biogenesis pathways in cancer. *Nat Rev Cancer*. 2015;15:321-333.
11. Peng Y, Croce CM. The role of microRNAs in human cancer. *Signal Transduct Target Ther.* 2016;1:15004.
12. Wu K, He J, Pu W, Peng Y. The role of exportin-5 in microRNA biogenesis and cancer. *Genomics Proteomics Bioinformatics.* 2018;16:120-126.
13. Sun HL, Cui R, Zhou J, et al. ERK activation globally downregulates miRNAs through phosphorylating exportin-5. *Cancer Cell.* 2016;30:723-736.
14. Li J, Pu W, Sun HL, et al. Pin1 impairs microRNA biogenesis by mediating conformation change of XPO5 in hepatocellular carcinoma. *Cell Death Differ*. 2018;25:1612-1624.
15. Zhou XZ, Lu KP. The isomerase PIN1 controls numerous cancer-driving pathways and is a unique drug target. *Nat Rev Cancer.* 2016;16:463-478.
16. Campaner E, Rustighi A, Zannini A, et al. A covalent PIN1 inhibitor selectively targets cancer cells by a dual mechanism of action. *Nat Commun.* 2017;8:15772.
17. Wei S, Kozono S, Kats L, et al. Active Pin1 is a key target of all-trans retinoic acid in acute promyelocytic leukemia and breast cancer. *Nat Med*. 2015;21:457-466.
18. Pu W, Li J, Zheng Y, et al. Targeting Pin1 by inhibitor API-1 regulates microRNA biogenesis and suppresses hepatocellular carcinoma development. *Hepatology.* 2018;68:547-560.
19. Moure MJ, SanMartin R, Dominguez E. Benzofurans from benzophenones and dimethylacetamide: copper-promoted cascade formation of furan O1-C2 and C2-C3 bonds under oxidative conditions. *Angew Chem Int Ed.* 2012;51:3220-3224.
20. Shen YD, Tian YX, Bu XZ, Gu LQ. Natural tanshinone-like heterocyclic-fused ortho-quinones from regioselective Diels-Alder reaction: synthesis and cytotoxicity evaluation. *Eur J Med Chem.* 2009;44:3915-3921.
21. Agasti S, Sharma U, Naveen T, Maiti D. Orthogonal selectivity with cinnamic acids in 3-substituted benzofuran synthesis through C-H olefination of phenols. *Chem Commun.* 2015;51:5375-5378.
22. Pu WC, Mu GM, Zhang GL, Wang C. Copper-catalyzed decarboxylative intramolecular *C*–O coupling: synthesis of 2-arylbenzofuran from 3-arylcoumarin. *RSC Adv*. 2014;4:903-906.
23. Zou Y, Yue G, Xu J, Zhou J. General Suzuki coupling of heteroaryl bromides by using tri- tert- butylphosphine as a supporting ligand. *Eur J Org Chem*. 2014;27:5901-5905.
24. Zeng W, Wu W, Jiang H, et al. Facile synthesis of benzofurans via copper-catalyzed aerobic oxidative cyclization of phenols and alkynes. *Chem Commun*. 2013;49:6611-6613.
25. Hsu SH, Wang B, Kota J, et al. Essential metabolic, anti-inflammatory, and anti-tumorigenic functions of miR-122 in liver. *J Clin Invest*. 2012;122:2871-2883.
26. Li Y, Cai B, Shen L, et al. MiRNA-29b suppresses tumor growth through simultaneously inhibiting angiogenesis and tumorigenesis by targeting Akt3. *Cancer Lett.* 2017;397:111-119.
27. Navarro E, Alonso SJ, Trujillo J, Jorge E, Pérez C. General behavior, toxicity, and cytotoxic activity of elenoside, a lignan from Justicia hyssopifolia. *J Nat Prod.* 2001;64:134-135.
28. Silva DHS, Pereira FC, Zanoni MVB, Yoshida M. Lipophyllic antioxidants from Iryanthera juruensis fruits. *Phytochemistry* 2001;57:437-442.
29. Cabibbo G, Latteri F, Antonucci M, Craxi A. Multimodal approaches to the treatment of hepatocellular carcinoma. *Nat Clin Pract Gastroenterol Hepatol.* 2009;6:159-169.
30. Llovet JM, Villanueva A, Lachenmayer A, Finn RS. Advances in targeted therapies for hepatocellular carcinoma in the genomic era. *Nat Rev Clin Oncol.* 2015;12:408-424.
31. Lu J, Getz G, Miska EA, Alvarez-Saavedra E, Lamb J, Peck DA. MicroRNA expression profiles classify human cancers. *Nature.* 2005;435:834-838.
32. Croce CM. Causes and consequences of microRNA dysregulation in cancer. *Nat Rev Genet*. 2009;10:704-714.
33. Kota J, Chivukula RR, O'Donnell KA, et al. Therapeutic microRNA delivery suppresses tumorigenesis in a murine liver cancer model. *Cell.* 2009;137:1005-1017.
34. Ling H, Fabbri M, Calin GA. MicroRNAs and other non-coding RNAs as targets for anticancer drug development. *Nat Rev Drug Discov.* 2013;12:847-865.
35. Jiang B, Pei D. A selective, cell-permeable nonphosphorylated bicyclic peptidyl inhibitor against peptidyl-prolyl isomerase Pin1. *J Med Chem.* 2015;58:6306-6312.